Characterizing Fiber Reinforced Polymer Composites Shear Behavior with Digital Image Correlation

QI AN, MATTHIAS MERZKIRCH and AARON M. FORSTER

ABSTRACT

The interlaminar and intralaminar shear properties, such as modulus and strength, are important for the design of fiber reinforced polymer (FRP) composite materials. Short beam strength is often used as a screening tool for interlaminar strength, whereas the V-Notched beam methods are considered valid for shear modulus and strength measurements. The advent of optical strain measurement techniques such as digital image correlation (DIC), provide new opportunities to generate high resolution maps of the shear strain field as a function of the globally applied strain. In this work, we show that non-contact measurements of the strain field are an important enhancement to measuring the shear properties of FRP composites. The V-Notched rail shear method is used to measure the shear modulus and strength of two different FRP composites that vary in reinforcement type (glass or carbon), matrix type (epoxy chemistry) and angle of the principle fiber axis to the shear loading axis. DIC was used to image the V-Notch-rail-method samples during shear measurement to track local strains and evaluate the shear strain across the gauge length and near the notch root in these specimens. The results are compared to analytical predictions of shear modulus derived from tensile properties of the epoxy polymer matrix and the reinforcing fiber.

INTRODUCTION

The accurate measurement of modulus and strength properties in tension, compression, and shear is the first step in the design of fiber reinforced polymer (FRP)

Qi An, Theiss Research, La Jolla, CA, 92037, USA; Materials Measurement Science Division, Material Measurement Laboratory, National Institute of Standards and Technology, Gaithersburg, MD 20899 USA
Matthias Merzkirch, Guest Researcher, Materials Science and Engineering Division, Material Measurement Laboratory, National Institute of Standards and Technology, Gaithersburg, MD 20899 USA
Aaron M. Forster, Materials Measurement Science Division, Material Measurement Laboratory, National Institute of Standards and Technology, Gaithersburg, MD 20899 USA

composite materials. The measurement of tension and compression properties is relatively straight-forward, but there are many different shear test methods (> 10 methods) for unidirectional and quasi-isotropic fiber reinforced composites. Each shear test method has its benefits, constraints and limitations with some better for interlaminar shear properties and others for intralaminar shear properties. One reason for so many choices is the difficulty in obtaining a reasonably pure and uniform shear stress state in the test specimen, which is critical if true shear properties are to be measured. The short beam strength test (ASTM 2344) [1] is a popular method for screening the apparent interlaminar strength of fiber composites. Unfortunately, it does not provide an accurate measure of interlaminar stiffness. Additional test methods that are not used as frequently include the double-notch shear test (ASTM D3846) [2] and the non-standardized 10° off-axis test. The V-notched beam test ('Iosipescu', ASTM D5379) [3] and V-Notched rail shear test (ASTM D5379) [4] use a "butterfly" shaped specimen that has been shown to generate a uniform shear stress across the gauge section, but this too is dependent on sample configuration and the shape of the V-Notch used to concentrate shear stresses in the gauge region. Regardless, these tests are applicable to obtaining shear stiffness and strength measurements for certain fiber orientations. In addition, these two methods are applicable for measuring the in-plane shear modulus properties as a function of longitudal fiber direction. The gauge length of the V-Notched rail specimen is 31 mm whereas that of the Iosipescu specimen is 11 mm. This increased gauge length induces a more uniform shear stress, has the potential for more accurate measures of shear stiffness, and has a higher probability of failure in the gauge section between the notches [5]. In this work, the V-Notched rail shear test was chosen to measure Low density (LD) unidirectional (UD) E-glass fabric and carbon fibr prepreg, epoxy based composites were utilized as test specimens. The orientation of the reinforcing fibers to the loading axis is varied to alter the shear stress distribution and strength of the material.

Distributions of shear strains were analyzed using digital image correlation (DIC) [6]. This technology is a topological non-contact material independent solution for full field determination of displacements, deformation and strain. Non-contact full field strain measurements provide access to local and global strain information. This paper provides an in-depth analysis of how optical strain methods are important for FRP material shear testing by comparing V-notch rail test responses from two different FRP composite materials, with DIC, in terms of shear strength, shear modulus, strain to failure, shear strain distributions and crack initiation.

EXPERIMENTAL

Materials and Composites Manufacturing

The material details and dimensions are given in Table I. LD E-glass UD fabric (Style 7721, Thayercraft Inc., USA) was used to make glass fiber-reinforced polymer (GFRP) composites. Approximately 15 % of the overall fabric mass are the stitching fibers which are aligned perpendicular to the UD fibers. These fibers are the same E-glass materials woven at a lower density than the UD fibers. Four plies of the as-received, LD E-glass UD fabric were infused with a stoichiometric ratio of EPON 862 and Epi-Kure W (Hexion Specialty Chemicals) using a vacuum-assisted resin transfer

molding process (VARTM). The UD fibers were kept in the same direction for all layers. Distribution media was applied to aid through thickness resin infusion. The double bag technique was utilized to facilitate a uniform infusion surface. The infusion of the vacuum-degassed resin occurred under full vacuum (- 100 kPa) and 55 °C using a flow media to aid through-thickness resin diffusion. Infusion took place over half an hour before final cure under full vacuum at 130 °C for 6 hours.

The unidirectional carbon fiber (DowAksa A-42, 24K) reinforced epoxy prepregs were formed by a sheet molding compound (SMC) process. These carbon fiber reinforced polymer (CFRP) composites were created by stacking twelve prepreg layers resulting in a thickness of the cured laminate sheet material of approximately 2.4 mm. The UD fibers were kept in the same direction for all layers.

In accordance with ASTM D5379, a loading angle of 0° correspond to longitudinal fiber alignment perpendicular to the loading direction, whereas a loading angle of 90° represents longitudinal fiber alignment parallel to the loading direction [4]. Nominal +45° is considered as counter-clockwise from the longitudinal fiber alignment.

TABLE I. SUMMARY OF MATERIAL TYPE AND DIMENSIONS OF THE TEST SPECIMENS. THE UNCERTAINTIES IN THE THICKNESS MEASUREMENT AND REINFORCING FRACTION ARE LISTED.

Materials	Nominal Fabric density (g/cm^3)	Thickness (mm)	Reinforcing fraction (mass %)	Loading Angles (°)	Number of fabric layers	Manufacturing method
UD E-glass (LD) - epoxy	2.03	0.93 ± 0.01	54.31 ± 0.35	90, 0, +45	4	VARTM
UD carbon - epoxy	1.78	2.40 ± 0.01	59.08 ± 0.31	90	12	prepreg

Thermogravimetric Analysis

The mass fraction of the reinforcing fibers and epoxy matrix materials in the FRP composites was measured via gravimetric analysis using a thermogravimetric analyzer. A temperature-ramp- isothermal-hold method [7] was used to thermally remove the organic components. The isothermal step temperature was 800 °C and 500 °C for the glass reinforcement and CFRP reinforcement, respectively. The reinforcing fiber mass fraction was approximately 54 % for the LD GFRP composite and 59% for the CFRP composite, estimated from thermogravimetric analysis (TGA) measurements.

Tensile Properties

Average quasi-static (strain rate of 0.0001 s^{-1}) Young's modulus (E), ultimate tensile strength (UTS), and strain to failure (ε_f) from uniaxial tensile testing of GFRP UD (LD) in the longitudinal direction, and of the matrix material is listed in Table II. Tensile testing is still ongoing, therefore, values from literature [8, 9, 10] have been taken for Poisson's ratios (v) of the composite in longitudinal direction as well as for the matrix material for the calculation of the matrix' shear modulus (G) via the following equation (only applicable for isotropic material):

$$G = \frac{E}{2(1+\nu)} \quad (1)$$

TABLE II: AVERAGE QUASI-STATIC (STRAIN RATE OF 0.0001 S^{-1}) RESULTS FROM UNIAXIAL TENSILE TESTING OF GFRP UD IN LONGITUDINAL (L) [11] AND TRANSVERSE (T) DIRECTIONS, AND OF THE MATRIX MATERIAL. THE UNCERTAINTIES IN MEASUREMENT, STANDARD DEVIATION ABOUT MEAN ARE LISTED.

	UTS (MPa)	E (GPa)	ν	ε_f (%)	G (GPa)
L	696.5 ± 30.5	31.1 ± 1.2	0.28 ± 0.01 (literature)	3.6 ± 0.8	Eq. (1) not applicable
T	measurements are underway				Eq. (1) not applicable
Epoxy (Matrix)	76.5 ± 2.14	2.6 ± 0.1	0.353 (literature)	4.5 ± 1.0	0.96 ± 0.04

Average quasi-static (strain rate of 0.0001 s^{-1}) results from uniaxial tensile testing of CFRP UD in longitudinal and transverse directions, and of the matrix material is listed in Table III. The degree of orthotropicity (E_L/E_T) is about 15 (6 %), representing a high anisotropy. The Young's modulus in the transverse direction is over two times the modulus of the matrix material.

TABLE III: AVERAGE QUASI-STATIC (STRAIN RATE OF 0.0001 S^{-1}) RESULTS FROM UNIAXIAL TENSILE TESTING OF CFRP UD IN LONGITUDINAL AND TRANSVERSE DIRECTIONS, AND OF THE MATRIX MATERIAL (TAKEN FROM INVESTIGATIONS FOLLOWED FROM [12]). THE UNCERTAINTIES IN MEASUREMENT, STANDARD DEVIATION ABOUT MEAN ARE LISTED.

	UTS (MPa)	E (GPa)	ν	ε_f (%)	G (GPa)
L	1846 ± 133	124 ± 1	0.33 ± 0.04	1.38 ± 0.10	Eq. (1) not applicable
T	66.0 ± 1.4	8.1 ± 0.3	0.02 ± 0.01	0.85 ± 0.07	Eq. (1) not applicable
Epoxy (Matrix)	75.3 ± 6.5	3.4 ± 0.1	0.38 ± 0.03	3.13 ± 0.59	1.22 ± 0.05

V-Notch Rail Test - Testing Setup and DIC Configuration

The V-Notch rail test [4] was used to measure the in-plane shear properties of GFRP and CFRP composites. The V-Notch rail fixture (Wyoming Test Fixtures Inc.) is shown in Figure 1 (left). The fixture clamps the face of the composite sample and shear is induced by parallel motion of the opposing clamp rail. Displacement controlled tests were conducted on an electromechanical machine at a nominal rate of 2 mm/min according to [4].

This design includes a multitude of degrees of freedom that enable flexibility in accommodating a variety of sample thicknesses, but requires careful alignment prior to testing. A precision steel block was used for rotational alignment of the left and right rails to reduce out-of-plane misalignment (Z-direction). The front grip face was aligned with a precision steel block so that the specimen is in the loading axis (X-Y plane) of

the test machine. According to [4] back-to-back two-element strain gauges are suggested to evaluate the degree of twist due to force eccentricity.

The testing was coupled with stereo DIC for visualization and quantification of different full-field behaviors (e.g., absolute displacements, strains and rotations) under shear loading within a free unsupported/unclamped area of approximately 28 mm, see Figure 1 (right). The fixture allows for DIC acquisition from both sides of the sample, here stereo DIC is used on one face of the sample to visualize out-of-plane deformation,

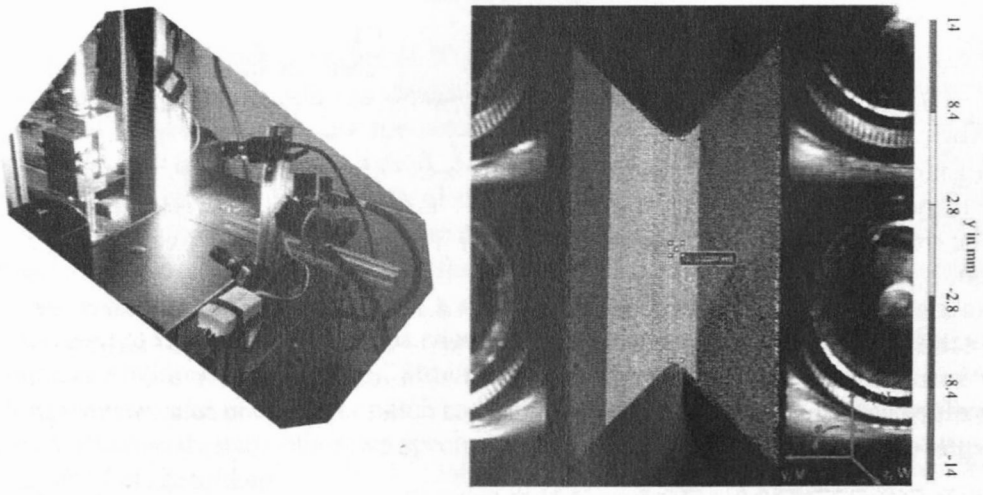

Figure 1: Testing setup and vertical positioning of the DIC acquisition systems (left), Field of View (FOV) and Region of interest (ROI), colored area (right).

All specimens were prepared for DIC measurements with commercially available matte white spray paint, followed by applying matte black spray paint to create a random pattern of speckles by an overspray method (indirect painting through placing specimen perpendicular to the spraying direction). For stereo-DIC measurements, two 5 Mpx (2448 x 2048) CCD cameras and 50 mm lenses have been used. As can be seen from Figure 1(left), a vertical position of the camera system has been chosen due to the small free unsupported area and the needed stereo angle (approximately 23°). The image acquisition rate was 3 Hz. The magnification was 36 µm per pixel and the size of the dark speckles was approximately 212 µm (approximately 6 px), measured via the line intersection method. The dark/bright ratio of the sample was almost equal (50:50). According to [6], the subset size of the image that will be analyzed should be at least three times the average speckle size, and the step size a third to a half the subset size. For data analysis, the chosen subset size was 25 px and the step size was 10 px. The reference image has been taken at a force F = 0 kN while the specimen has only been clamped by the right grip. For analysis, engineering strain is calculated using a commercially available DIC software package.

RESULTS AND DISCUSSION

Figure 2 shows the evolution of the maximum shear strain γ_{12} calculated via the principal strains ε_1 and ε_2:

$$\varepsilon_{12} = \frac{\varepsilon_1 - \varepsilon_2}{2} = {}^1/_2\,\gamma_{12} \tag{1}$$

$$\gamma_{12} = \varepsilon_1 - \varepsilon_2 \tag{2}$$

for specimens with loading angles of 0° (left), 90° (middle) and +45° (right). In the equations, the strains depicted are chosen at an average shear strain of approximately 0.6 % in the central area between the notch roots (where the width of the gauge length is narrowest, see ROI Figure 1 (right)). According to [4], the use of specialized shear strain gauges, which span the length of the test section between the notch roots, are recommended. A benefit of optical strain measurements is the ability to characterize an average shear strain even with a nonuniform shear stress state present across the gauge section.

As can be seen from Figure 2, the shear strain distribution is non-uniform between the notches for the tested specimens. Strain concentrations at the notch roots can be seen for 0° specimens and at the lower notch root. The 90° specimen shows a more uniform strain distribution than the other two specimens and with a shear strain concentration in the center of the specimen.

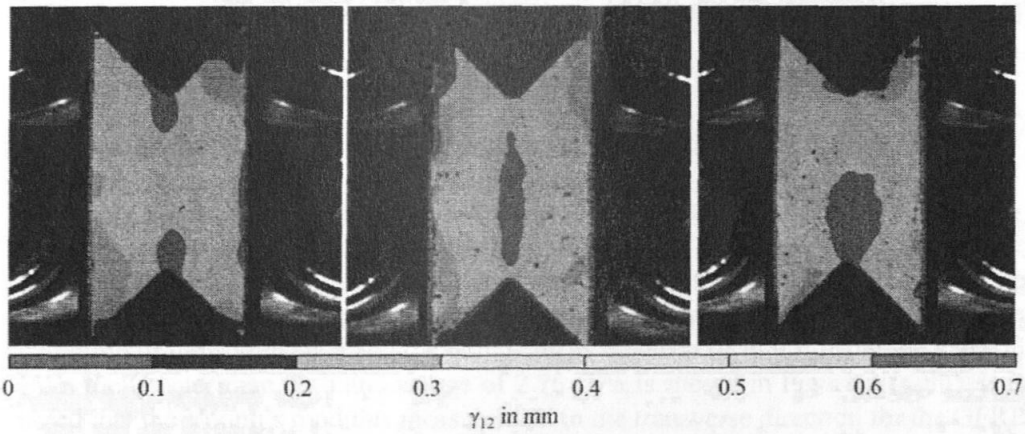

Figure 2: Evolution of maximum shear strains for different loading directions at an average strain of 0.6 %: 0° (left), 90° (middle), +45° (right).

To model the evolution of the shear stress τ, the following equation was used:

$$\tau = \frac{F}{w \cdot th} \tag{3}$$

both stress and strain consistently refer to the notched gauge section with width (w) and thickness (th). Figure 3 (left) depicts the shear stress-shear strain curves up to failure of the specimen tested in directions 0°, 90°, and +45°. The maximum shear strength of the specimens tested at a loading angle of 90° is approximately 45 MPa at a strain to failure of approximately 4.0 %.

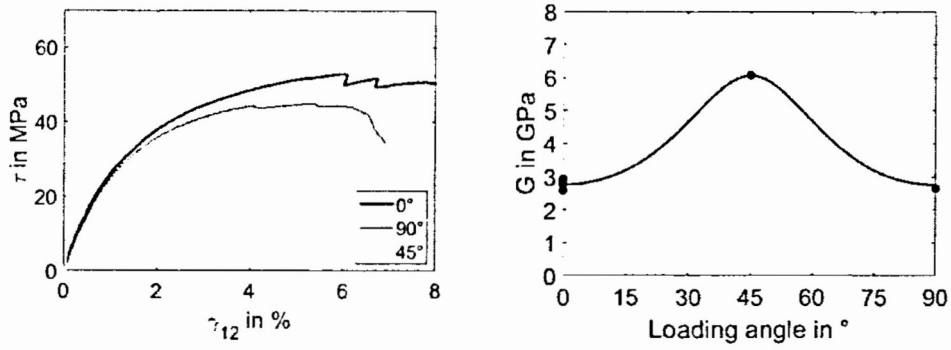

Figure 3: Shear stress- shear strain curve until fracture for specimens tested in directions 0°, 90°, and +45° (left). Evolution of shear modulus along loading direction (right). The uncertainty in the measurement for G_{12}(0°) was +/- 0.17 GPa.

According to [3, 4, 13], the shear modulus for composites can be extracted when the average shear strain ranges between 0.2 % ± 0.05 % to 0.6 % ± 0.05 %. Figure 3 (left) shows the shear stress vs. shear strain of the specimens tested in the fiber orientation for loading angles of 90°, 45° and 0°. Furthermore, the compliance in shear is expressed by [14]:

$$S_{66} = \frac{\cos^2 2\varphi}{G_{12}} + \left(\frac{1}{E_L} + \frac{1}{E_T} + 2 \cdot \frac{\upsilon_L}{E_L}\right) \cdot \sin^2 2\varphi \qquad (4)$$

where S_{66} is the engineering shear compliance, G_{12} is the transverse shear modulus, E_L is the tensile modulus in the longitudinal fiber direction, E_T is the tensile modulus in the transverse fiber direction, υ_L is the Poisson's ratio parallel to the fiber direction, φ is the loading angle. The parameters needed for equation (4) are taken from Table II. The evolution of the compliance along loading angles between 0° to 90° using the value G from the 0° specimen with an average of 2.76 GPa is shown in Figure 3 (right). It is noted that the Young's modulus measurement in the transverse direction for the GFRP is in progress. In the absence of this data, the curve for equation 4 is fitted to the modulus at a loading angle of 45° and assuming a Young's Moduli for the transverse direction of 8.7 GPa.

Figure 4 depicts the out-of-plane deformation, W, at the maximum force. All configurations show a ΔW up to 2 mm. The magnitude of W is affected by the alignment of the wedge, clamping pressure, and the length-to-thickness ratio of the gauge length of the sample.

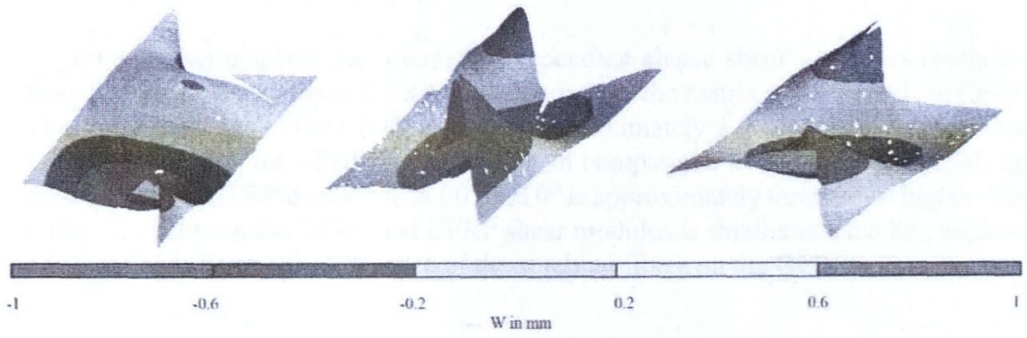

Figure 4: Out-of-plane deformation for different loading directions at maximum force: 0° (left), 90° (middle), +45° (right). The scale bar shows the magnitude of W (mm).

Corresponding fractography of LD UD GFRP composites for different loading directions is shown in Figure 5, white arrows indicate fiber directions. The 0° (Figure 5(a)) and +45° (Figure 5(c) and 5(d)) specimens show a transverse fracture far from the notch root, consequently the maximum shear stresses (reference the top of the notched area) depicted in Figure 3 (right) do not represent failure stresses within the gauge length. The 90° (Figure 5(b)) specimen shows failure at or near the notch root which can also indicate significant transverse strains.

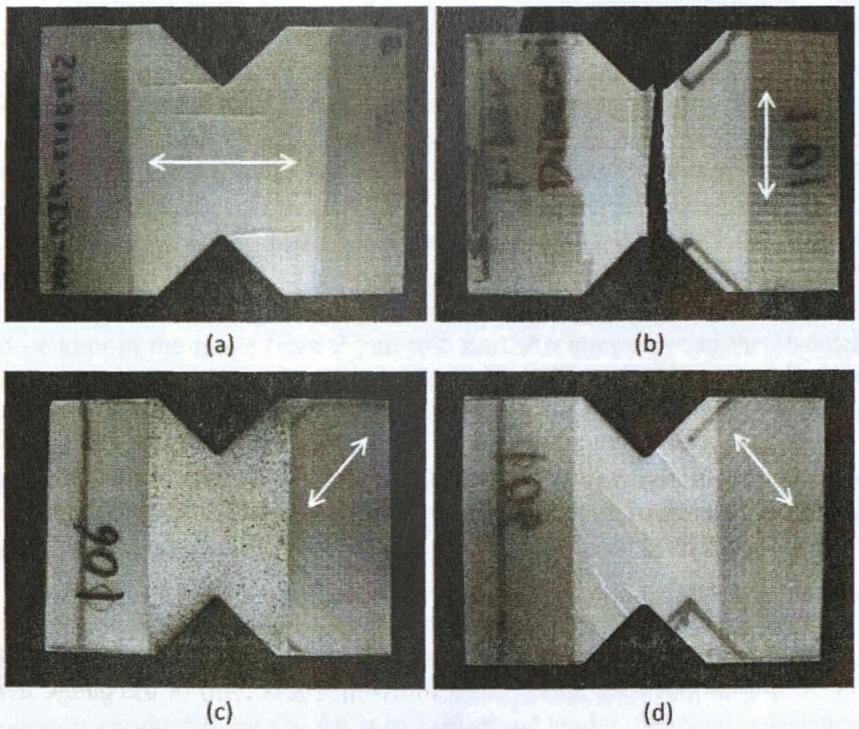

Figure 5: Fractography of LD UD GFRP composite for different loading directions: (a) 0°; (b) 90°; (c) +45° front side; (d) +45° back side showing fracture patterns. The arrows indicate the principle fiber directions.

CONCLUSIONS AND OUTLOOK

Figure 6 summarizes the orientation dependent elastic shear properties (outgoing from 0°) for the epoxy based GFRP in comparison to the matrix material and the CFRP. The shear modulus of the CFRP system is approximately 1.5 GPa (50%) higher than the shear modulus for GFRP at 0° and 90°. In comparison to the matrix material, the modulus of the GFRP composite at 90° and 0° is approximately three times higher. The difference between the GFRP and CFRP shear modulus is smaller at a loading angle of +45°, which indicates the influence of the stitching fibers on the GFRP.

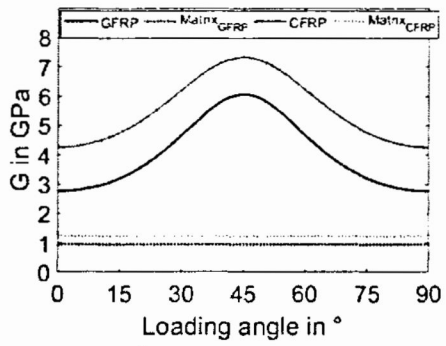

Figure 6: Evolution of the shear moduli over the loading angle for CFRP in comparison to the isotropic epoxy matrix material and CFRP.

The DIC measurements indicate a more symmetric strain field across the gauge section for 90° specimens than for the 0° and +45° specimens at an average strain of 0.6 % within the notched area and. At 0°, strain concentrations exist at the notch root and, at +45° a non-uniform strain field exists thus indicating the influence of the fiber orientation. The extraction of the shear strain between the notch roots allows for accounting for the strain inhomogeneity in the shear modulus calculation.

In terms of shear strength, all specimens show a mixed mode failure that includes the intended Mode II failure, as well as Mode I due to transverse stresses and Mode III due to twisting and buckling of the specimen. Accoridng to [4], the specimen thickness should be kept in the range from 2 mm to 5 mm. An alternative to the V-notched rail test method for specimens with a small thickness could be the V-notched beam method [3], where the actual length is smaller and therefore buckling of the specimen may be reduced.

Future research will focus on the determination of the quasi-static tensile properties using DIC in order to perform a sensitivity analysis on the shear properties presented within the current work.

ACKNOWLEDGMENTS

Research conducted by Qi An was performed under financial assistance award (Grant #70NANB16H202) from the U.S. Department of Commerce, National Institute of Standards and Technology. Qi An would like to acknowledge Ajay Krishnamurthy

for help with TGA measurements on fiber volume fractions of composites. Matthias Merzkirch is sponsored by NIST Guest Researcher program. The work on CFRP was carried out under the ICME Development of Carbon Fiber Composites for Lightweight Vehicles project directed by Ford Motor Company and funded by the U.S. Department of Energy under contract number DE-EE0006867. We would also like to thank Edward Pompa for waterjet cutting the specimens and Louise A. Powell for providing the results of the uniaxial tensile tests on CFRP.

DISCLAIMER

Certain commercial equipment and/or materials are identified in this report in order to adequately specify the experimental procedure. In no case does such identification imply recommendation or endorsement by the National Institute of Standards and Technology, nor does it imply the equipment and/or materials used are necessarily the best available for the purpose.

REFERENCES

1. ASTM Standard D2344/D2344M, 2016, " Standard Test Method for Short-Beam Strength of Polymer Matrix Composite Materials and Their Laminates," *ASTM International*, West Conshohocken, PA, 2016, DOI: 10.1520/D2344_D2344M-16, www.astm.org.
2. ASTM Standard D3846, 2008 (2015), "Standard Test Method for In-Plane Shear Strength of Reinforced Plastics," *ASTM International*, West Conshohocken, PA, 2015, DOI: 10.1520/D3846-08R15, www.astm.org.
3. ASTM Standard D5379/D2344M, 2012, "Standard Test Method for Shear Properties of Composite Materials by the V-Notched Beam Method," *ASTM International*, West Conshohocken, PA, 2012, DOI: 10.1520/D5379_D5379M-12, www.astm.org.
4. ASTM Standard D7078/D7078M, 2012, "Standard Test Method for Shear Properties of Composite Materials by V-Notched Rail Shear Method," *ASTM International*, West Conshohocken, PA, 2012, DOI: 10.1520/D7078_D7078M-12, www.astm.org.
5. Adams, D., *A Comparison of Shear Test Methods*. CompositesWorld, 2009. Available from: https://www.compositesworld.com/articles/a-comparison-of-shear-test-methods.
6. iDICs. *A Good Practices Guide for Digital Image Correlation*. 2017; Available from: http://idics.org/guide/.
7. Bücheler, D., A. Kaiser, and F. Henning, "Using Thermogravimetric Analysis to Determine Carbon Fiber Weight Percentage of Fiber-Reinforced Plastics," *Compos., Part B: Eng.*, 2016. 106: p. 218-223.
8. Bunsell A.R., *Fibre Reinforcements for Composite Materials*, Composite Materials Series 2, Elsevier, 1994.
9. Peters S.T., *Handbook of Composites*, Second Edition, Chapman & Hall, 1997.
10. Ishai O., *Engineering mechanics of composite Materials*, Oxford University Press, 1994.
11. An, Q., Tamrakar, S., Gillespie, J.W., Rider, A.N. and Thostenson, E.T., 2018. "Tailored glass fiber interphases via electrophoretic deposition of carbon nanotubes: Fiber and interphase characterization," *Composites Science and Technology, https://doi.org/10.1016/j.compscitech.2018.01.003*
12. Powell, L.A., et al., "High Strain Rate Mechanical Characterization of Carbon Fiber Reinforced Polymer Composites Using Digital Image Correlations," *SAE International Journal of Materials and Manufacturing*, 2017. **10**(2): p. 138-146.
13. ASTM Standard D3518/D3518M, 2013, " Standard Test Method for In-Plane Shear Response of Polymer Matrix Composite Materials by Tensile Test of a ±45° Laminate," *ASTM International*, West Conshohocken, PA, 2015, DOI: 10.1520/D3518_D3518M-13, www.astm.org.

14. Schürmann, 2007 #135 Schürmann, Helmut. *Konstruieren Mit Faser-Kunststoff-Verbunden. Konstruieren Mit Faser-Kunststoff-Verbunden*. Springer, 2007. doi:10.1007/978-3-540-72190-1.